Flood, R.D., Piper, D.J.W., Klaus, A., and Peterson, L.C. (Eds.), 1997
Proceedings of the Ocean Drilling Program, Scientific Results, Vol. 155

14. *DATA REPORT:* ENVIRONMENTAL ROCK-MAGNETIC EVIDENCE OF AUTHIGENIC-MAGNETIC MINERAL FORMATION/PRESERVATION (AMAZON FAN)[1]

Frank R. Hall,[2] Stanley Cisowski,[3] and Suku John[4]

ABSTRACT

Environmental rock-magnetic analyses were performed on sediments from all 17 sites drilled during Ocean Drilling Program Leg 155, Amazon Fan (Sites 930–946). In addition to the particles delivered to these sites via mass-wasting processes, rock-magnetic signals indicate the presence of authigenic magnetic-mineral phases. In particular, these phases include bacterial magnetite (Fe_3O_4) and greigite (Fe_3S_4).

INTRODUCTION

Environmental rock-magnetic analyses (Thompson and Oldfield, 1986) were performed on samples from all 17 sites drilled during Ocean Drilling Program (ODP) Leg 155 (Fig. 1). These data indicate the relative changes in concentration, grain size, composition, and grain alignment of magnetic minerals within the sediment. Numerous articles have been written that explain how such data are interpreted (e.g., Thompson and Oldfield, 1984; Hall and King, 1989; Roberts, 1995). The reader is referred to these articles and to Table 1 for further explanation.

In addition to these analyses, paleomagnetic results (see Cisowski and Hall, this volume), the anisotropy of magnetic susceptibility (AMS) of silt layers (see Hiscott et al., this volume), and the magnetic hysteresis parameters of magnetic Fe-sulfide nodules (see Hall et al., this volume) are reported elsewhere.

METHODS

The samples used in these measurements include those collected during and after the cruise. Post-cruise sampling was performed only on the top 100 m of sediments from these sites.

Samples were collected by insertion of standard ODP plastic paleomagnetic cubes (volume = 7 cm^3) into the split-face of the working half. Samples were commonly exhumed by insertion of a nonmagnetic stainless steel spatula underneath the cube. The bottom portion of the sample was removed, and the exteriors of the cubes were cleaned using dry paper toweling prior to placing the cap onto the cubes. Orientation was maintained with respect to the up-core (-Z) direction.

Discrete samples were measured for magnetic susceptibility using the Bartington Instruments System and are reported in volume-corrected units. Anhysteretic remanent magnetizations (ARM: peak AC field = 99.9 mT, DC field = 0.1 mT) were then applied using a

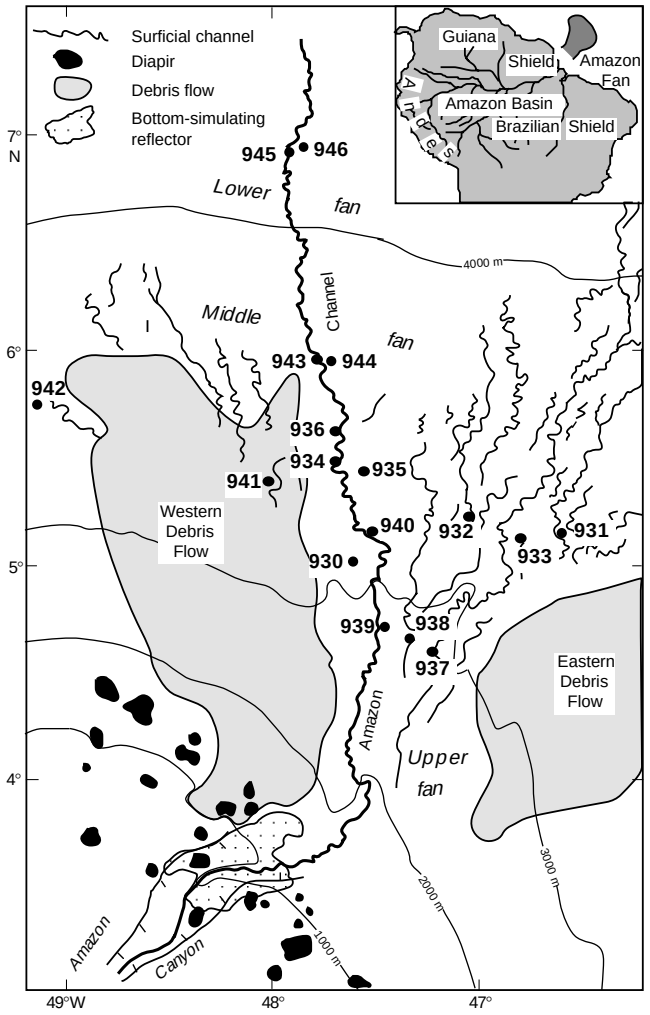

Figure 1. The locations of the Amazon Fan and Leg 155 drill sites. Map from Flood, et al., 1995; modified from Damuth et al. (1988) and Manley and Flood (1988).

[1]Flood, R.D., Piper, D.J.W., Klaus, A. and Peterson, L.C. (Eds.), 1997. Proc. *ODP, Sci. Results*, 155: College Station, TX (Ocean Drilling Program).
[2]Graduate College of Marine Studies, University of Delaware, Newark, DE 19716, U.S.A. frhall@udel.edu
[3]Department of Geological Sciences, University of California Santa Barbara, Santa Barbara, CA 93105, U.S.A.
[4]Department of Geological Sciences, University of Delaware, Newark, DE 19716, U.S.A.

Previous Chapter | Table of Contents | Next Chapter

Table 1. The interpretation of rock-magnetic parameters used in this text and the units for data reported here.

Parameter	Interpretation	Relative values		SI units volume corrected values
		High	Low	
K (susceptibility)	Concentration	High[a]	Low	10^{-11} SI
$IRM_{1.2T}$	Concentration	High	Low	A/m
K_{ARM}/K	Concentration (also affected by grain size)	High	Low	10^{-11} SI
K_{ARM}/K	Grain size	Fine	Coarse	Unitless
$K_{ARM}/IRM_{1.2T}$	Grain size	Fine	Coarse	m^3/mA
SIRM/K	Grain size	Fine	Coarse	mA/m^3
HIRM	Hematite[b] concentration	High	Low	A/m
$S_{-0.1T}$	Coercivity[c]	High	Low	Unitless
$S_{-0.3T}$	Magnetite[d]/hematite concentration ratio	Higher magnetite	Higher hematite	Unitless

[a] For example, if the susceptibility values are high, the magnetic-mineral concentration is considered high.
[b] Canted-antiferromagnetic minerals.
[c] This parameter is not a direct measure of coercivity. We use this as a way of indicating how the actual coercivity values should change downcore.
[d] Ferrimagnetic minerals.

DTECH PARM coil linked to a Schoenstedt GSD-1 AF demagnetizer. ARMs were converted to anhysteretic susceptibility (KARM) by dividing the sample intensity with that of the DC field intensity (79.6 A/m = 0.1 mT). Because of later difficulties with the demagnetizer, ARMs were only performed on samples collected during the cruise. Isothermal remanent magnetizations (IRM) were then applied using an ASC Impulse magnetizer at 1.2 T followed by reverse field applications at –0.1 and –0.3 T. ARM and IRM were measured using a MOLSPIN magnetometer. These data are presented as volume-corrected values.

The relative concentrations of the canted-antiferromagnetic components are calculated by the parameter $HIRM_{-0.3T}$ using the equation:

$$HIRM_{-0.3T} = (IRM_{1.2T} + IRM_{-0.3T})/2$$

The "S" parameters ($S_{-0.1T}$ and $S_{-0.3T}$) were calculated using the equation:

$$S_{-0.1,\ 0.3T} = -(IRM_{-0.1,\ 0.3T}/IRM_{1.2T})$$

RESULTS

The rock-magnetic data show evidence of authigenic magnetic mineral phases within lithologic Units I and II ("Amachron" Units Am and Br; upper Pleistocene [Flood, Piper, Klaus, et al., 1995]). With the exception of Site 939, these data are from the same holes used for presenting the whole-core magnetic susceptibility data within the *Initial Reports* volume for this leg (Flood, Piper, Klaus, et al., 1995). The environmental rock-magnetic data collected are presented in Figures 2 through 18 and in Table 2, on CD-ROM in the back pocket of this volume.

The topmost sediment (Unit I) of these sites consists of a brown foraminiferal-nannofossil mud that is commonly <1 m thick. The rock-magnetic signature of these sediments consists of low magnetic-mineral concentration (K and $IRM_{1.2T}$) and high magnetic-mineral grain size (K_{ARM}/K and $K_{ARM}/IRM_{1.2T}$) parameters (e.g., Fig. 2). These data indicate low magnetic-mineral concentrations accompanied by very fine-grained magnetic particles, probably associated with the formation of bacterial magnetite (Fe_3O_4; see Cragg et al., this volume).

Most sites contain an underlying sedimentary unit (Subunit IIA) that typically consists of fine-grained clayey-silty muds. High $IRM_{1.2T}/K$ values indicate the presence of greigite (Fe_3S_4; Roberts, 1995; Hall et al., this volume). These high $IRM_{1.2T}/K$ data are usually accompanied with high $S_{-0.3T}$ and low HIRM and $S_{-0.1T}$ values. These data reflect the higher relative coercivity, fine grain size, and the increased proportion of the ferrimagnetic component in these sediments.

Greigite is also found deeper in the holes, below Unit II. Using the criteria of relatively high $IRM_{1.2T}/K$ and $S_{-0.3T}$ coupled with relatively low HIRM and $S_{-0.1T}$ values, evidence of greigite formation, for example, can be seen at Site 930 (~142 mbsf and from ~202 mbsf to the base of the site; Fig. 2), and Site 942 (~65–75 mbsf; Fig. 14). Within debris flows, these data suggest greigite development at Site 931 (~83 and 305–360 mbsf; Fig. 3) and Site 933 (~165 to 190 mbsf; Fig. 5).

DISCUSSION

The dominant process of sedimentation on the Amazon Fan is mass wasting, primarily during glacial periods in the form of turbidity flows (Flood, Piper, Klaus, et al., 1995). Therefore, the overall magnetic mineralogy of these sediments should reflect the Amazon Basin source of these particles (see McDaniel et al., this volume). However, at least two authigenic phases of magnetic minerals can be detected using the environmental rock-magnetic techniques.

High K_{ARM}/K values within the top meter of sediment (lithologic Unit I) reflect the presence of bacterial magnetite (see Cragg et al., this volume). In addition, high $IRM_{1.2T}/K$ values, particularly within lithologic Unit II/IIA, reflect the presence of the greigite (see Hall et al., this volume). However, the presence of these minerals does not affect either the remanent magnetic signal (Cisowski et al., this volume) or the anisotropy of magnetic susceptibility (AMS) (Hiscott et al., this volume).

This result is contrary to the suggestion by Reynolds et al. (1994) that greigite can be the primary mineral giving rise to the paleomagnetic signal of sediments. There are at least two possible explanations for this result: (1) the total amount of terrigenous magnetic particles is sufficiently high that reduction diagenesis has minimal effect on the overall magnetic signature; or (2) the authigenic particles are not aligned with the magnetic field but have random orientations. This issue cannot be resolved with the data available.

CONCLUSIONS

From these analyses, we conclude that authigenesis and reduction diagenesis produce both magnetic Fe oxides and sulfides. The presence of these minerals can easily be detected using environmental rock-magnetic techniques. They do not directly affect the paleomagnetic signature of these sediments, however.

ACKNOWLEDGMENTS

We would like to thank Ms. Stefanie Reed for performing some of these measurements. We also thank personnel at the ODP Sample repository in Bremen, Germany, in particular, Mr. Walter Hale, for

their assistance during post-cruise sampling. Finally, we thank Drs. Roger Flood and David Piper, the co-chief scientists of this leg. This project was funded by USSAC Award No. 155-20846b.

REFERENCES

Damuth, J.E., Flood, R.D., Knowsmann, R.O., Belderson, R.H., Gorini, M.A., 1988. Anatomy and growth patterns of Amazon deep-sea fan as revealed by long-range side-scan sonar (GLORIA) and high-resolution seismic studies. *AAPG Bull*., 72:885–911.

Flood, R.D., et. al., 1995. Introduction. *In* Flood, R.D., Piper, D.J.W., Klaus, A., et al., *Proc. ODP, Init. Repts.*, 155: College Station, TX (Ocean Drilling Program), 5–16.

Flood, R.D., Piper, D.J.W., Klaus, A., et al., 1995. *Proc. ODP, Init. Repts*., 155: College Station, TX (Ocean Drilling Program).

Hall, F.R., and King, J.W., 1989. Rock-magnetic stratigraphy of Site 645 (Baffin Bay) from ODP Leg 105. *In* Srivastava, S.P., Arthur, M.A., Clement, B., et al., *Proc. ODP, Sci. Results*, 105: College Station, TX (Ocean Drilling Program), 843–859.

Manley, P.L., and Flood, R.D., 1988. Cyclic sediment deposition within the Amazon deep-sea fan. *AAPG Bull*., 72:912-925.

Reynolds, R.L., Tuttle, M.L., Rice, C.A., Fishman, N.S., Karachewski, J.A., and Sherman, D.M., 1994. Magnetization and geochemistry of greigite-bearing Cretaceous strata, North Slope Basin, Alaska. *Am. J. Sci.*, 294:485–528.

Roberts, A.P., 1995. Magnetic properties of sedimentary greigite (Fe_3S_4). *Earth Planet. Sci. Lett.*, 134:227−236.

Thompson, R., and Oldfield, F., 1986. *Environmental Magnetism:* London (Allen and Unwin).

Date of initial receipt: 1 December 1995
Date of acceptance: 13 June 1996
Ms 155SR-215

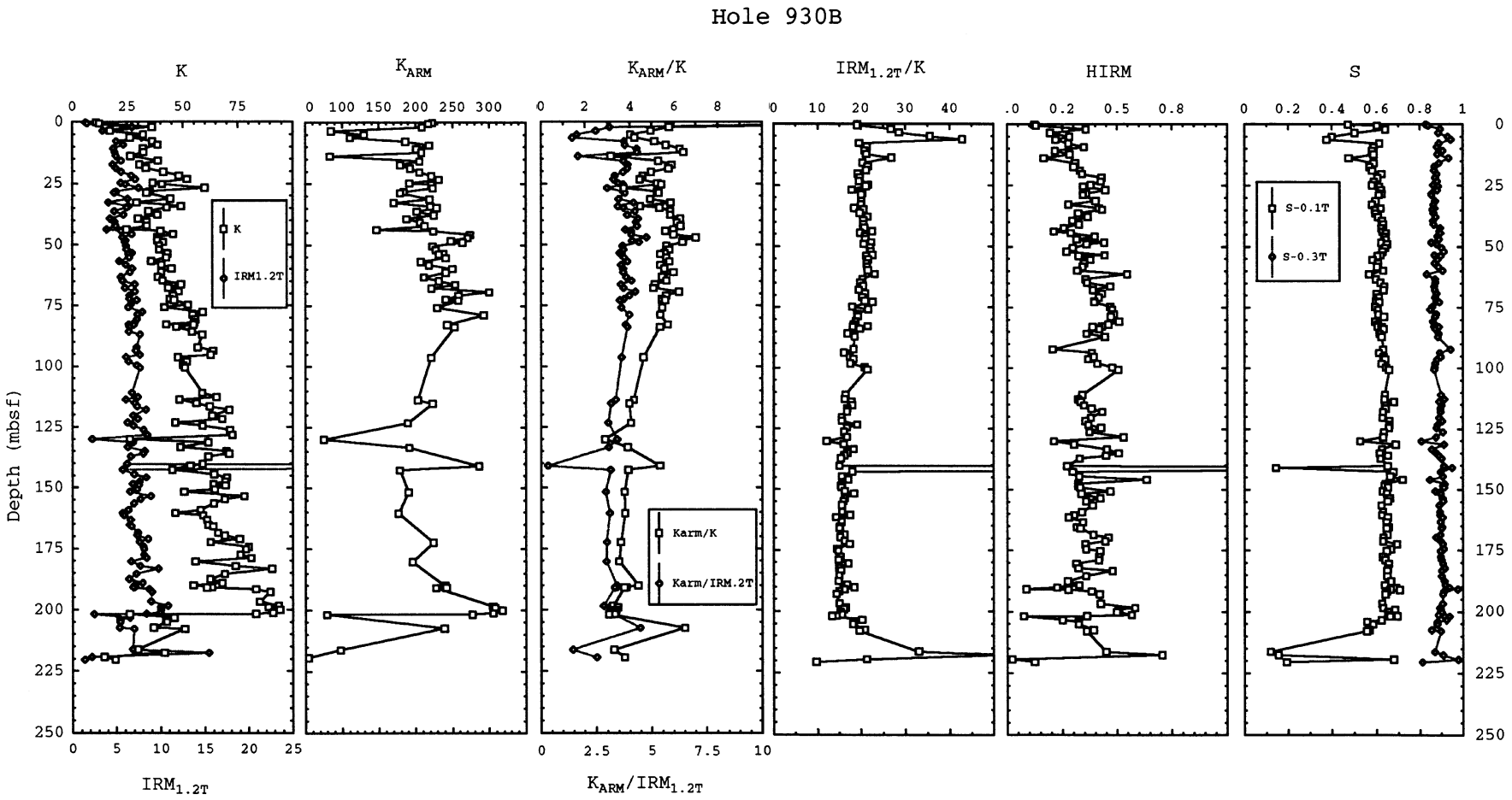

Figure 2. The environmental rock-magnetic data from Site 930.

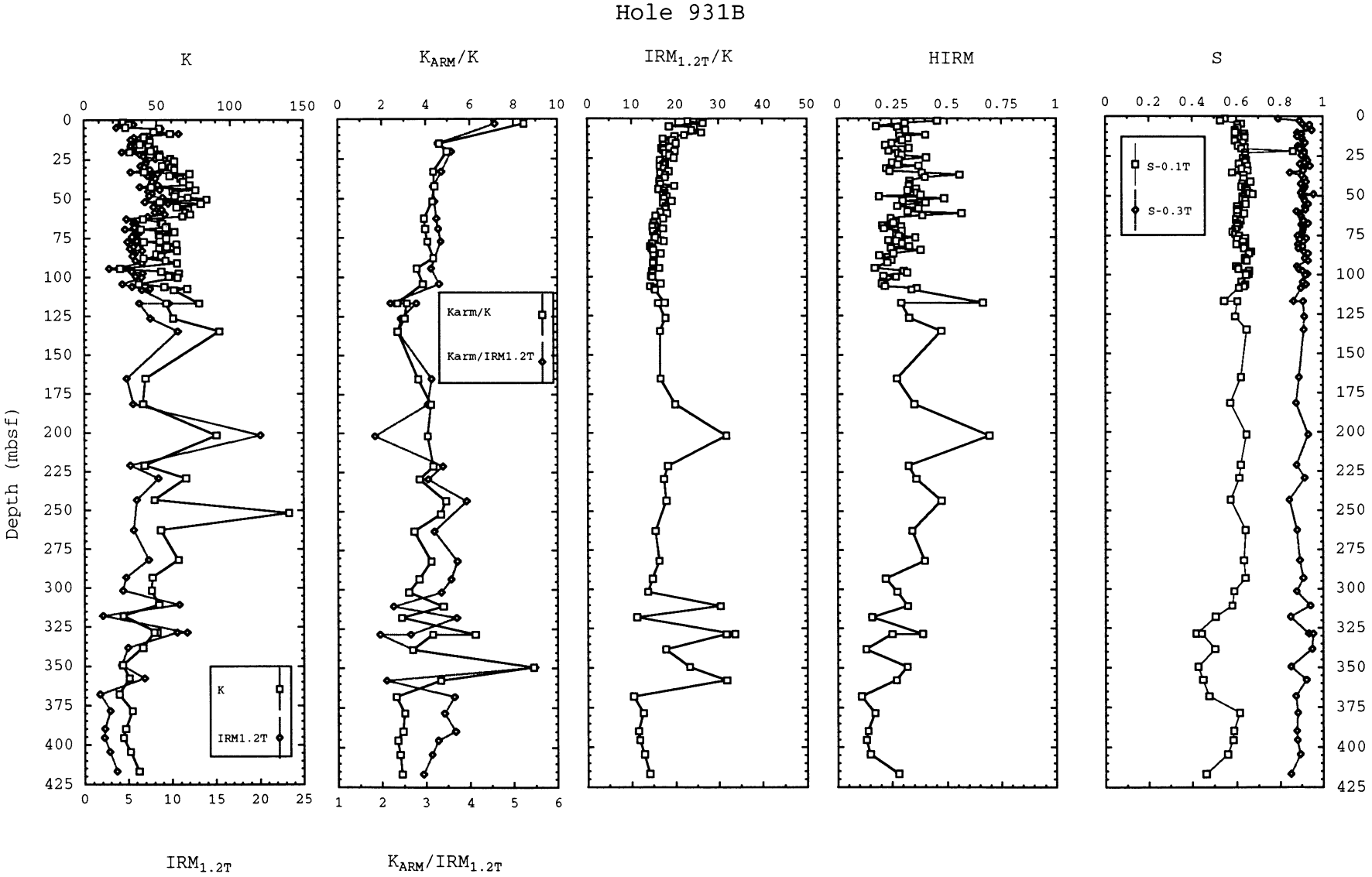

Figure 3. The environmental rock-magnetic data from Site 931.

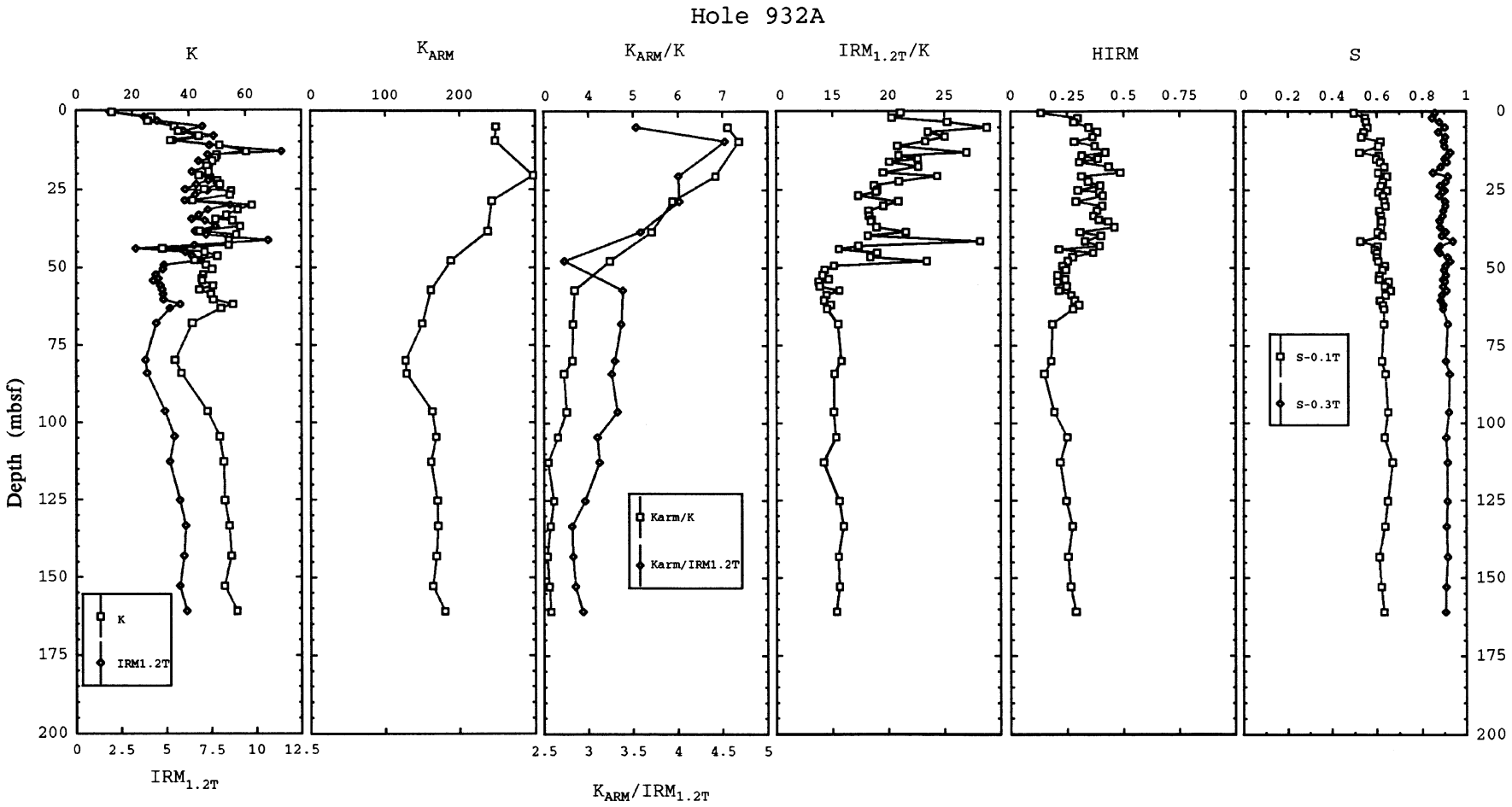

Figure 4. The environmental rock-magnetic data from Site 932.

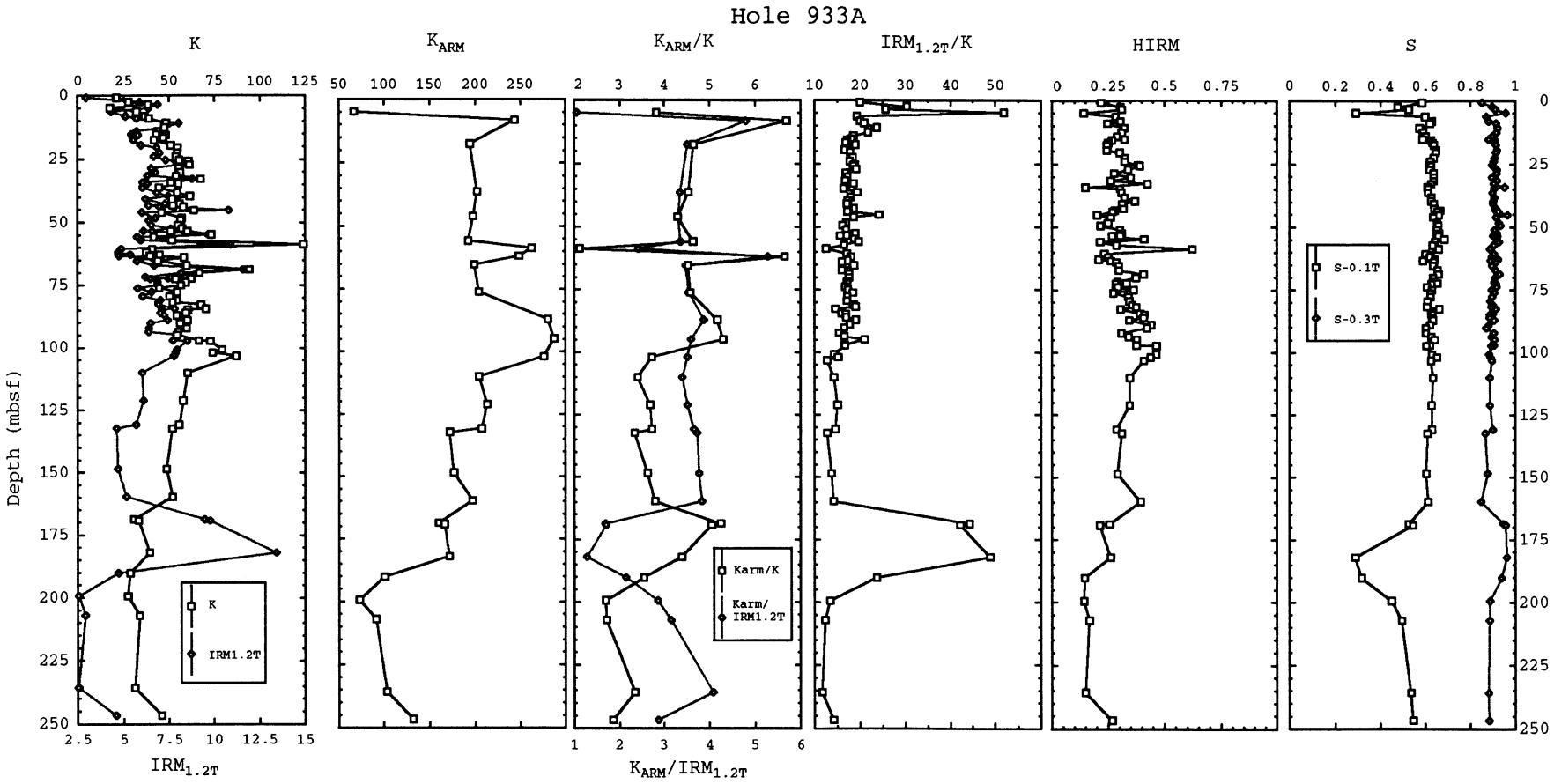

Figure 5. The environmental rock-magnetic data from Site 933.

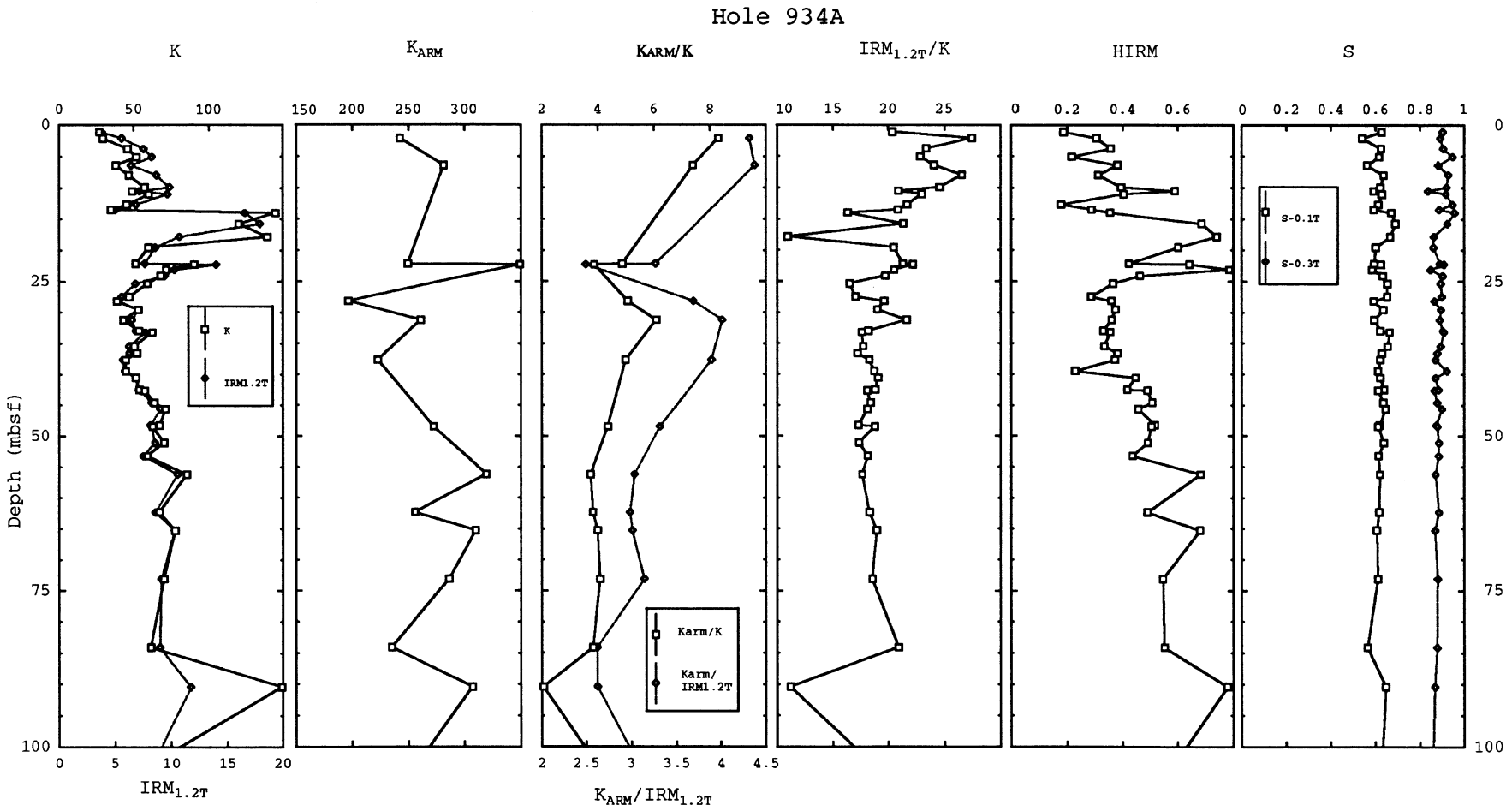

Figure 6. The environmental rock-magnetic data from Site 934.

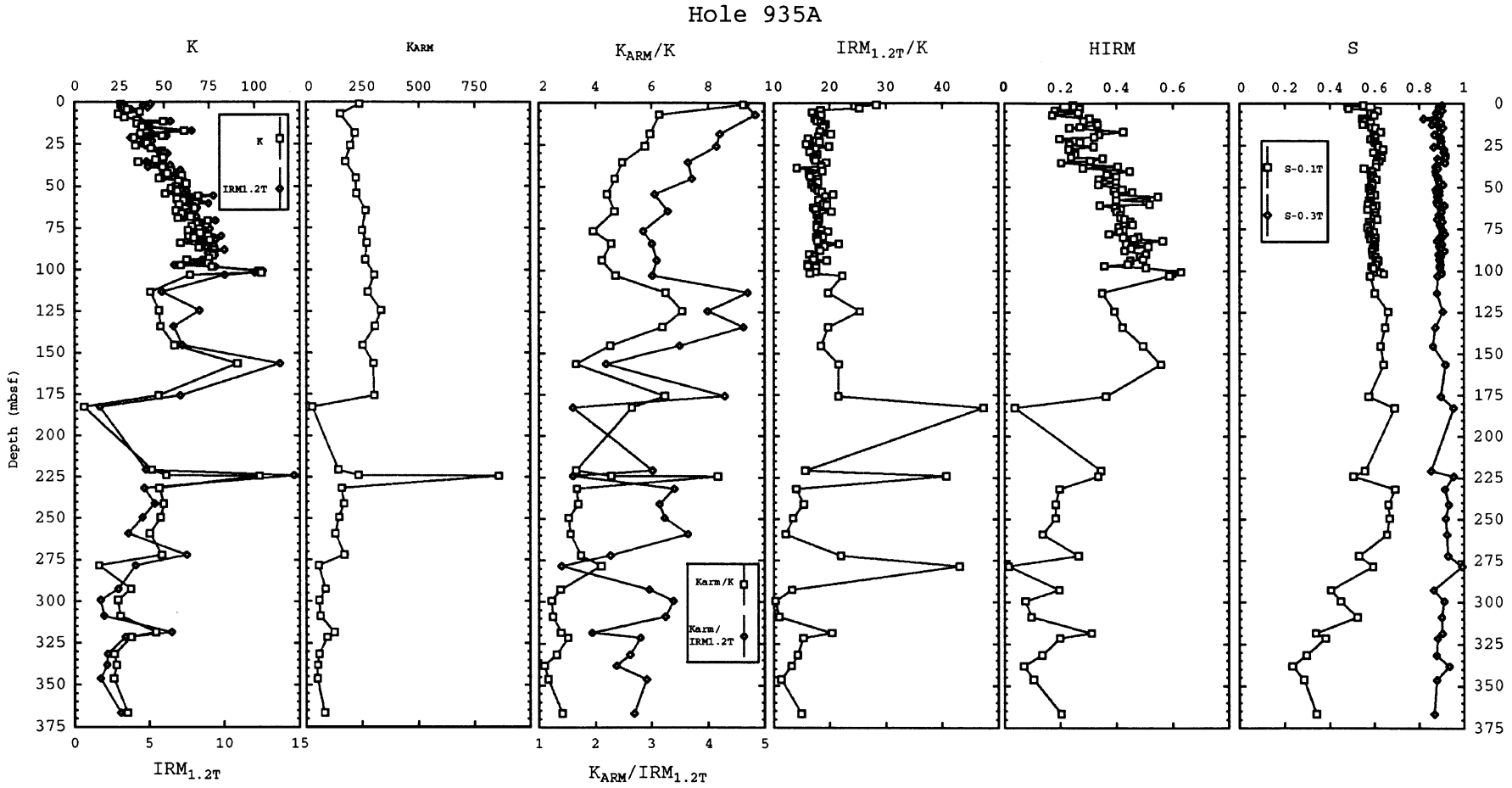

Figure 7. The environmental rock-magnetic data from Site 935.

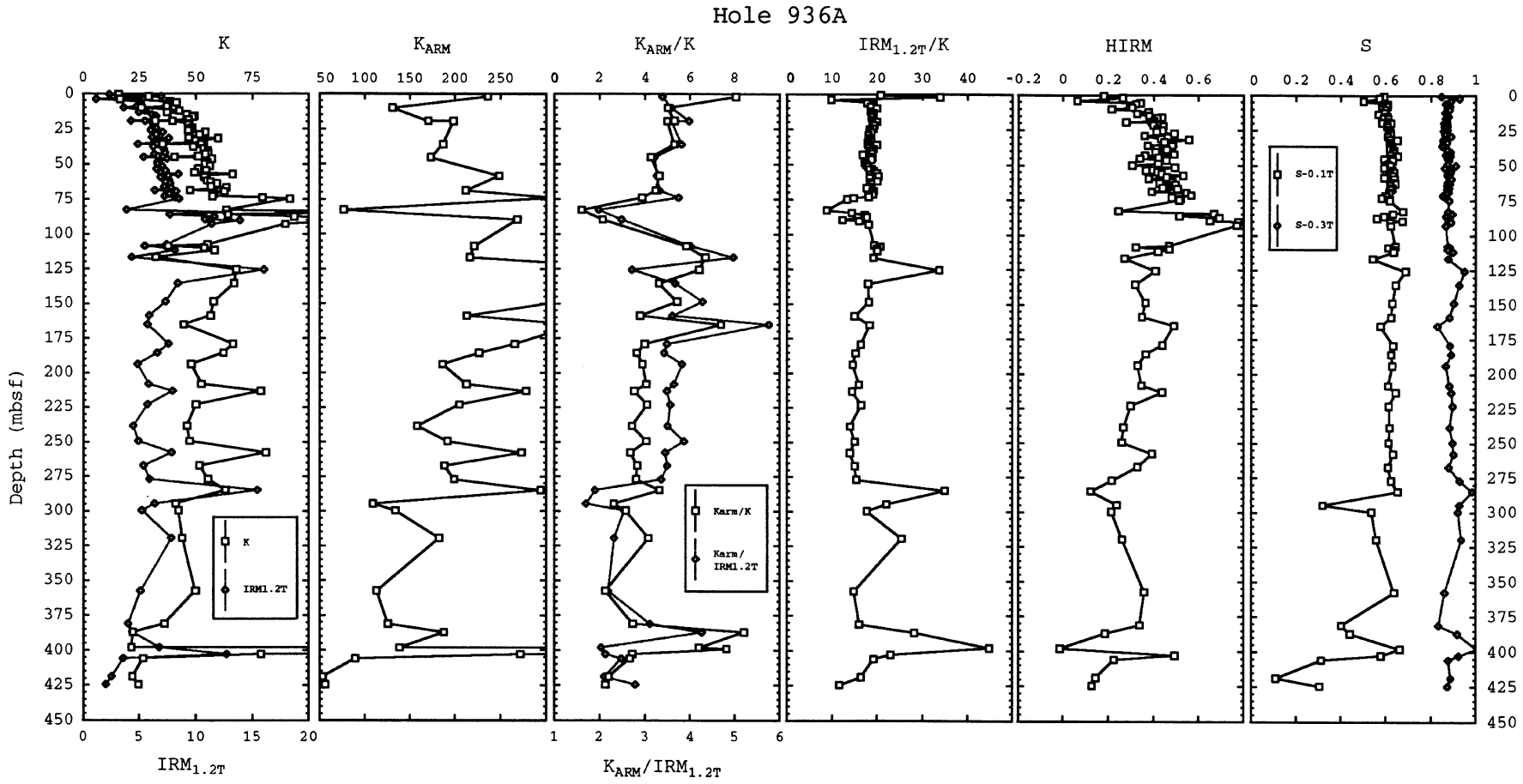

Figure 8. The environmental rock-magnetic data from Site 936.

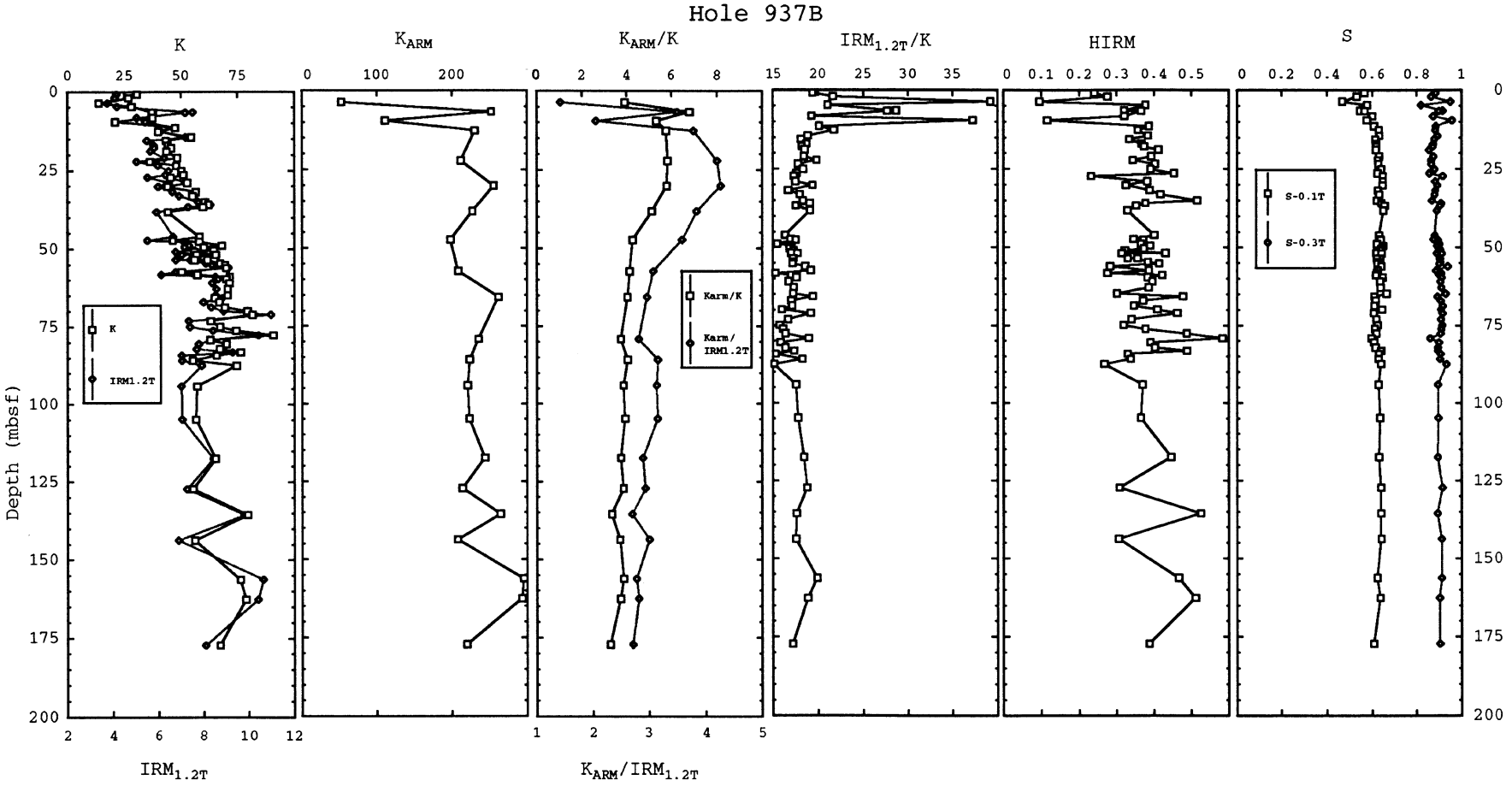

Figure 9. The environmental rock-magnetic data from Site 937.

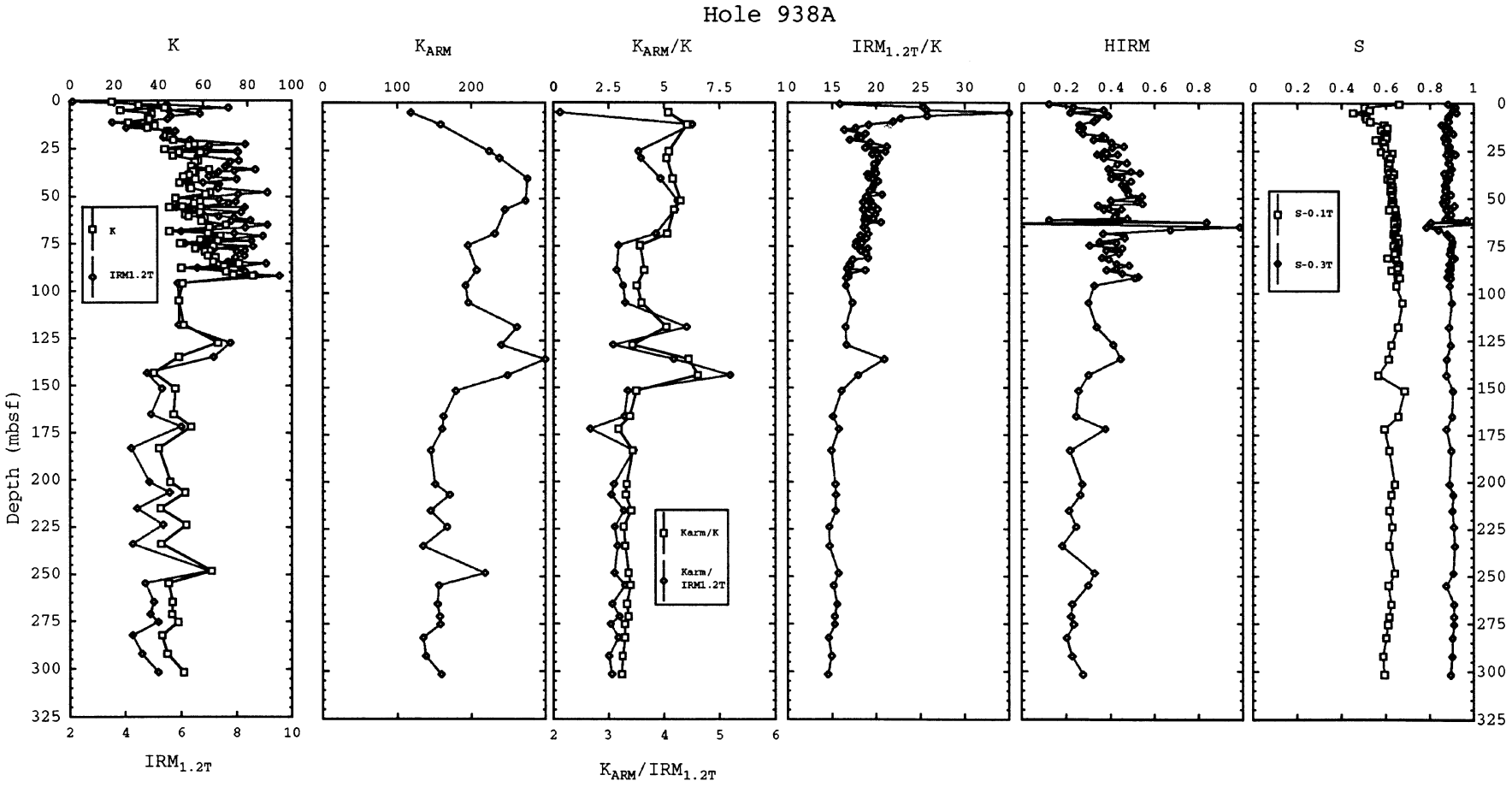

Figure 10. The environmental rock-magnetic data from Site 938.

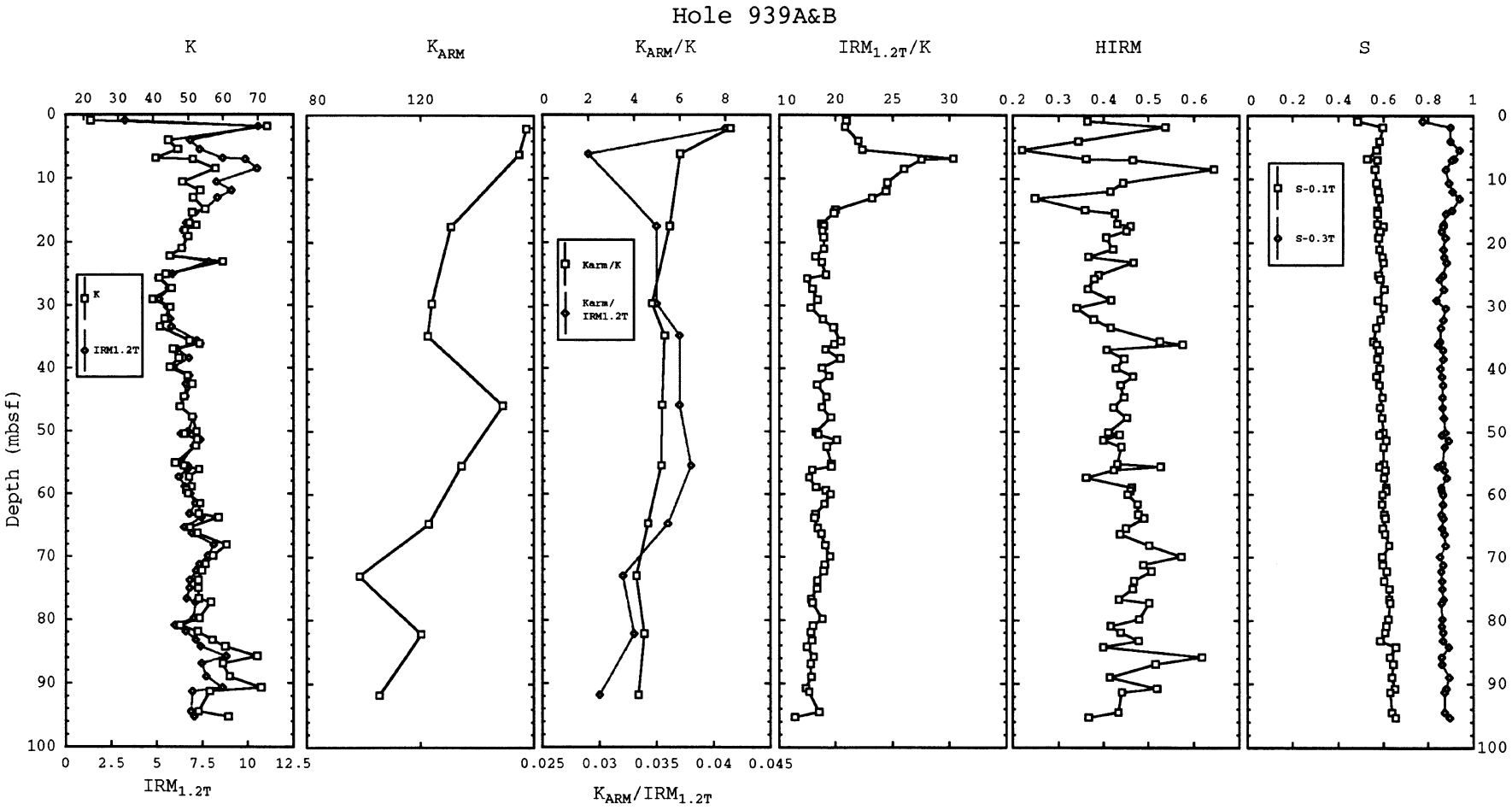

Figure 11. The environmental rock-magnetic data from Site 939.

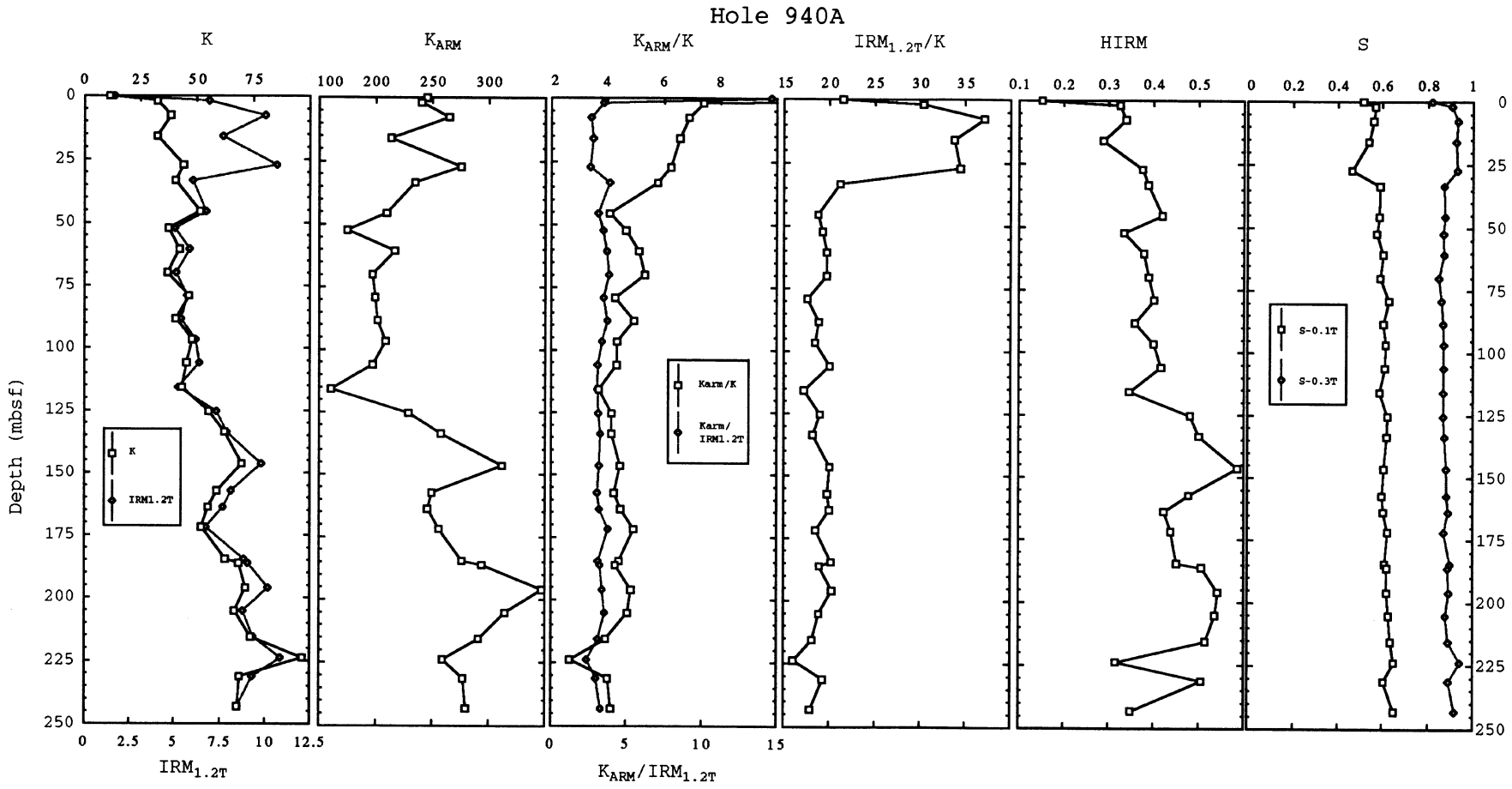

Figure 12. The environmental rock-magnetic data from Site 940.

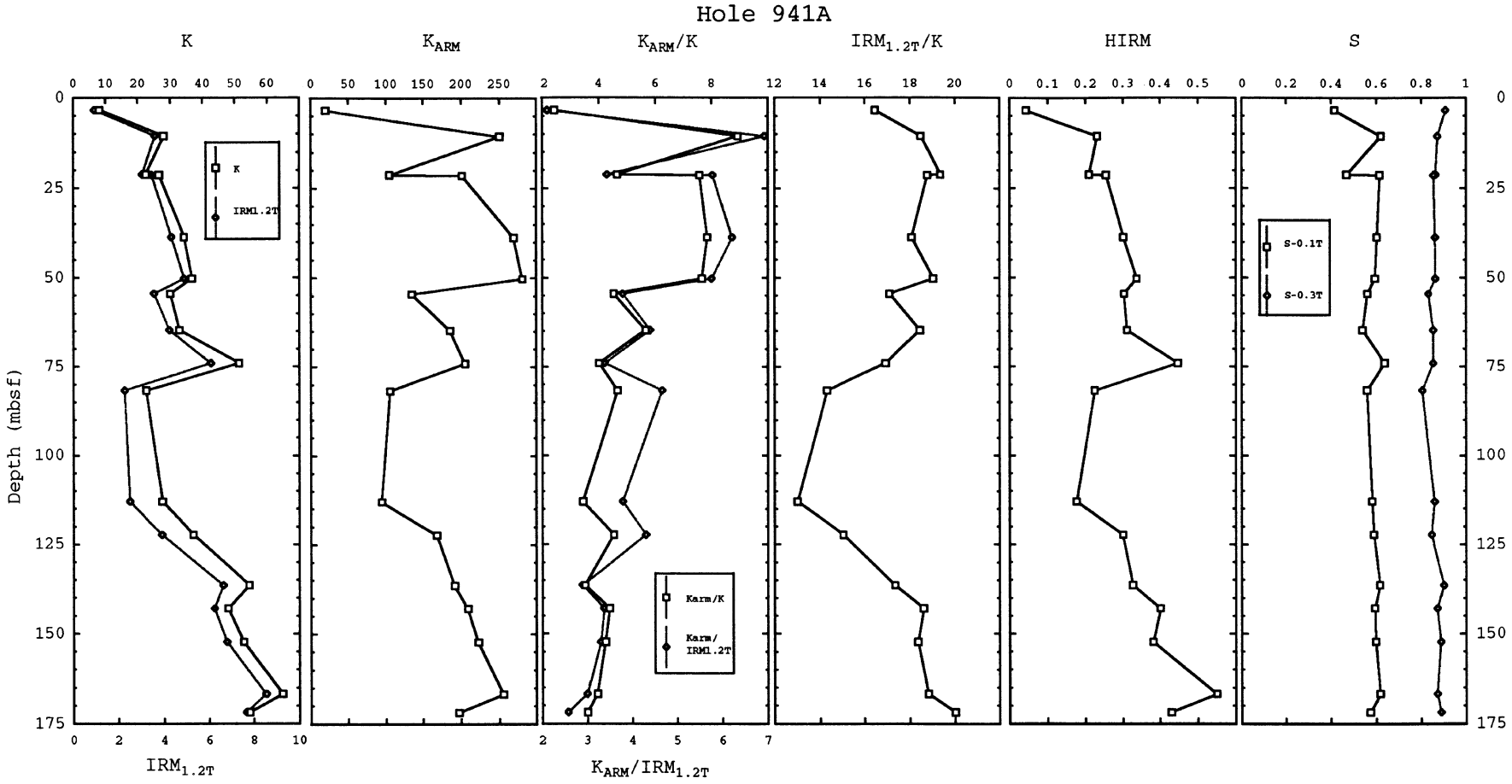

Figure 13. The environmental rock-magnetic data from Site 941.

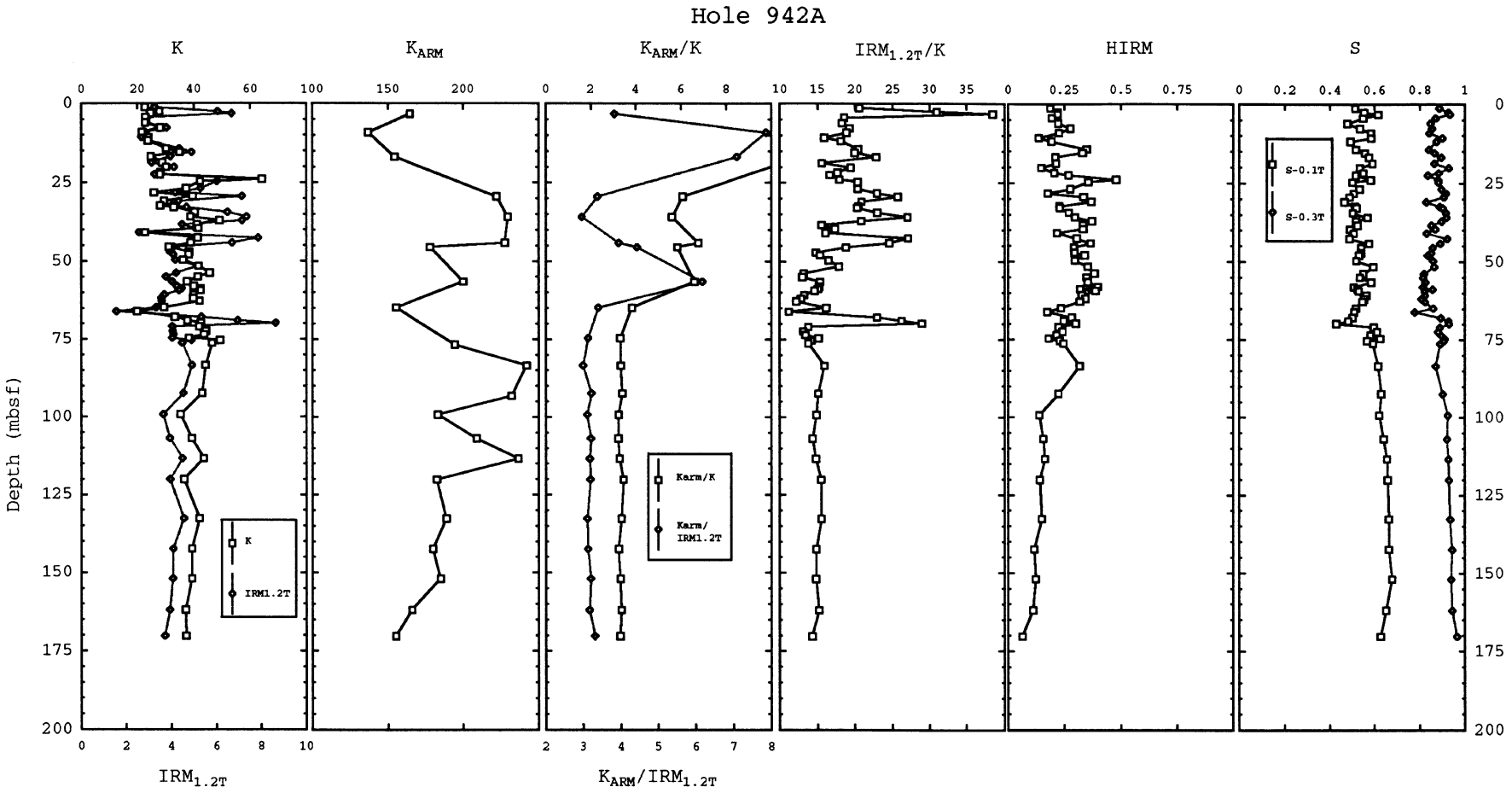

Figure 14. The environmental rock-magnetic data from Site 942.

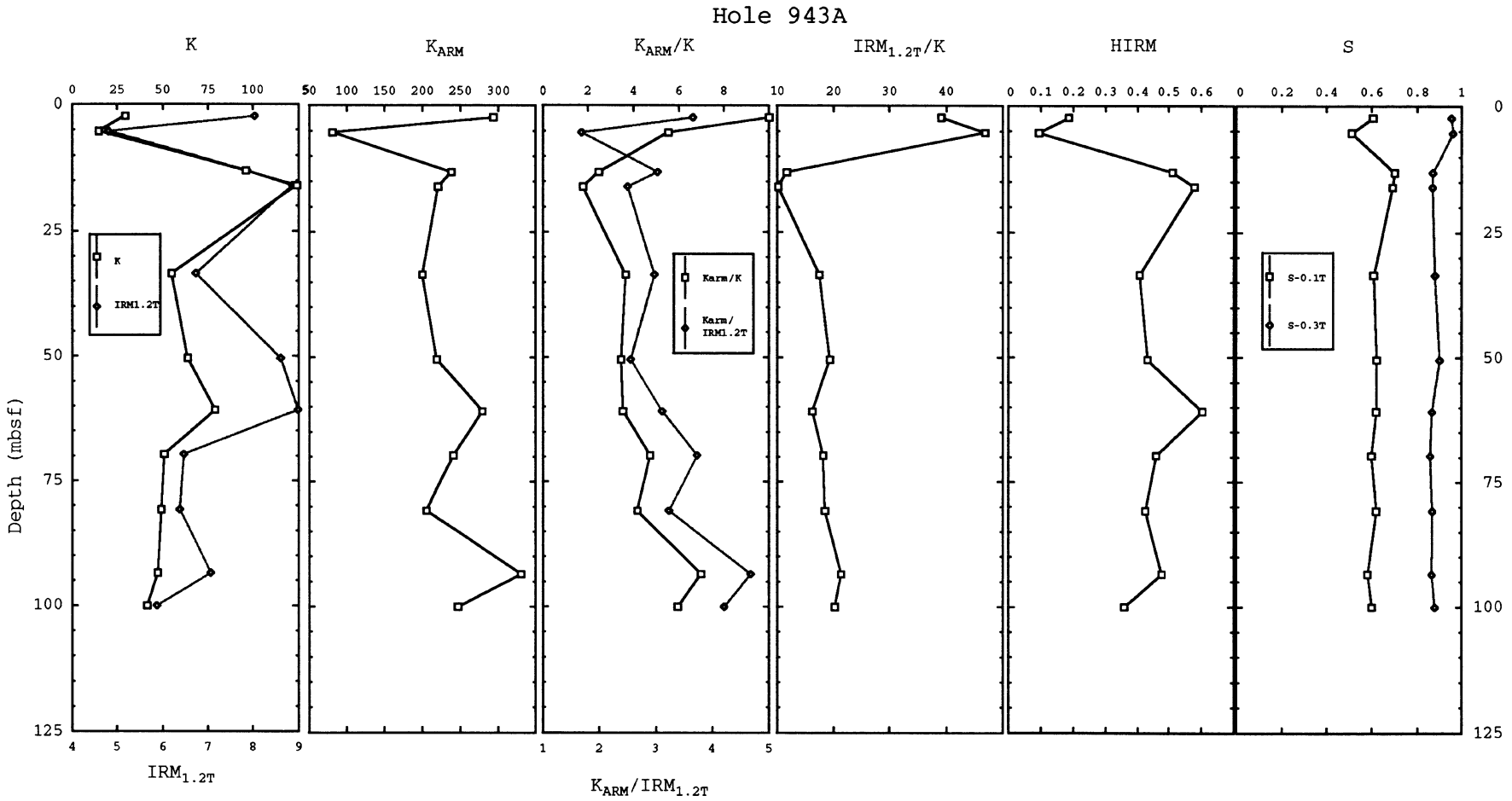

Figure 15. The environmental rock-magnetic data from Site 943.

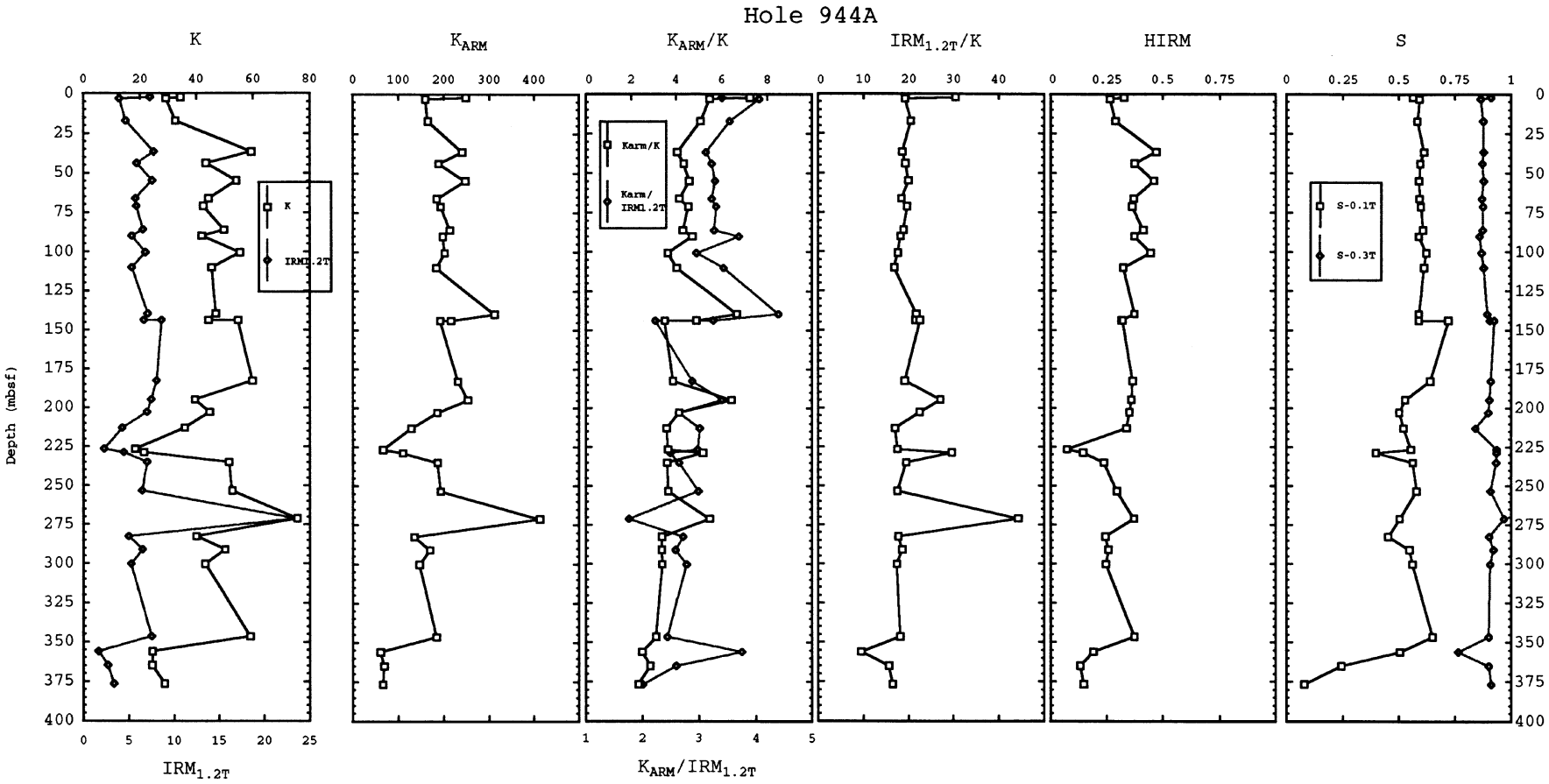

Figure 16. The environmental rock-magnetic data from Site 944.

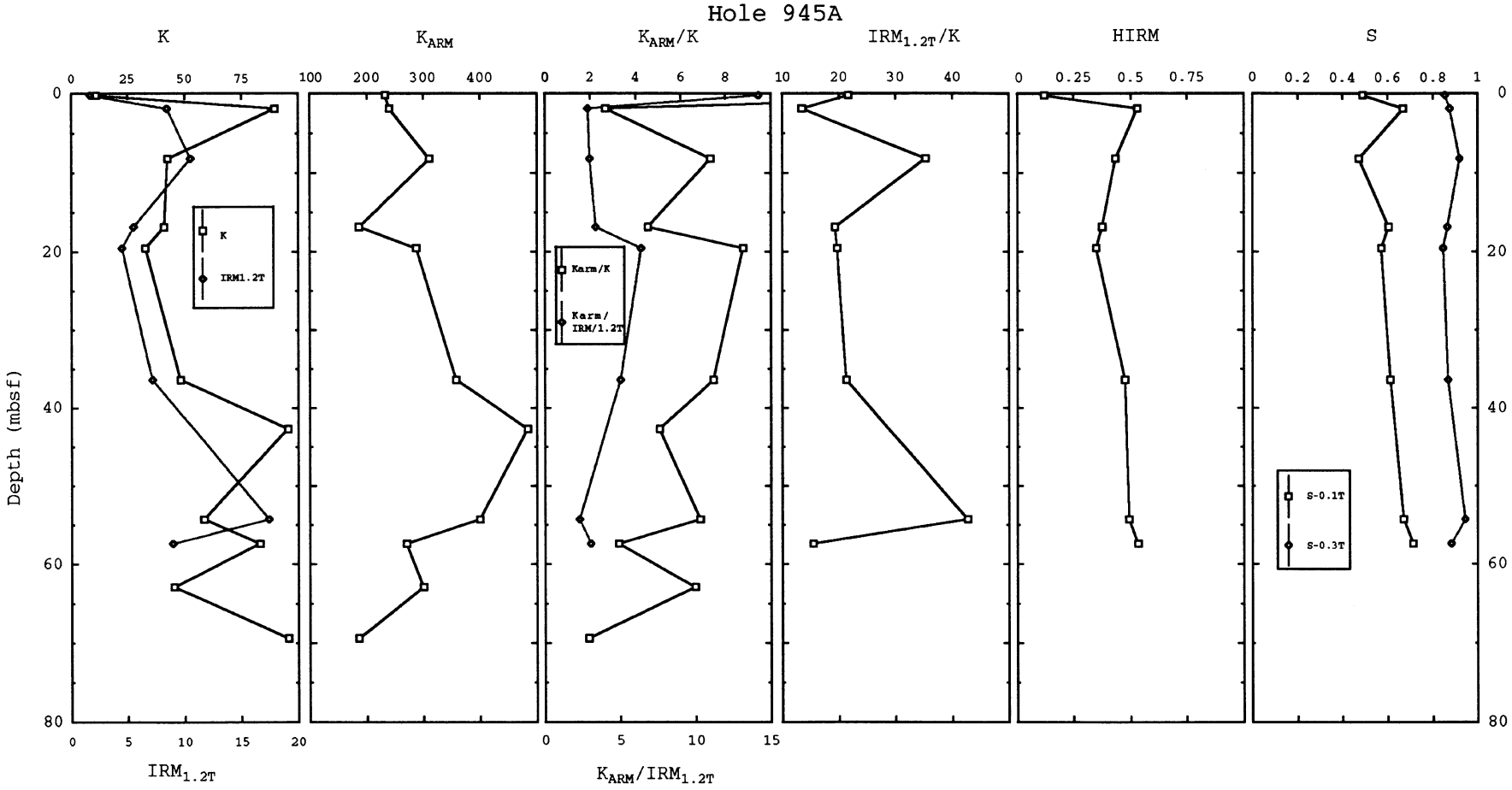

Figure 17. The environmental rock-magnetic data from Site 945.

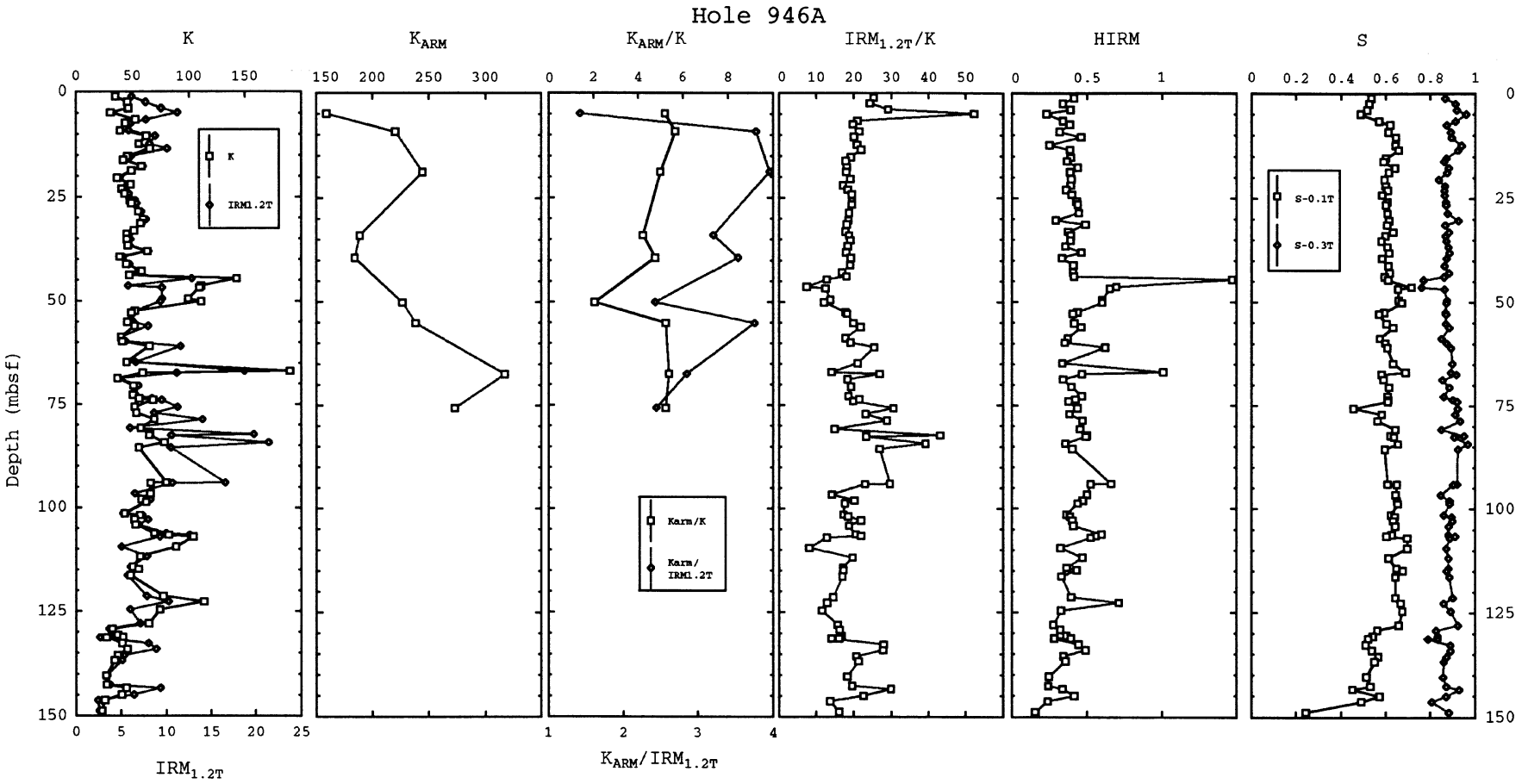

Figure 18. The environmental rock-magnetic data from Site 946.

Previous Chapter Table of Contents Next Chapter